Electronic supplementary information

Syngas-derived hydrophilic nanocarbon for water purification

Boborahimov Azamat Boborahim Ugli, Takeshi Fujita, Shusaku Shoji, Kako Tetsuya, Hideki Abe

[a] National Institute for Materials Science, Namiki 1-1, Tsukuba, Ibaraki 305-00443, Japan.
[b]Graduate School of Science and Engineering, Saitama University, Shimo-Okubo 255, Saitama 338-8570, Japan
[c] Tsukuba University, 1-chome-1-1 Tennodai, Tsukuba, Ibaraki 305-8577, Japan
[d] Institute of Materials and Systems for Sustainability, Nagoya University, Furo-cho,Chikusa-ku, Nagoya 464-8601, Japan

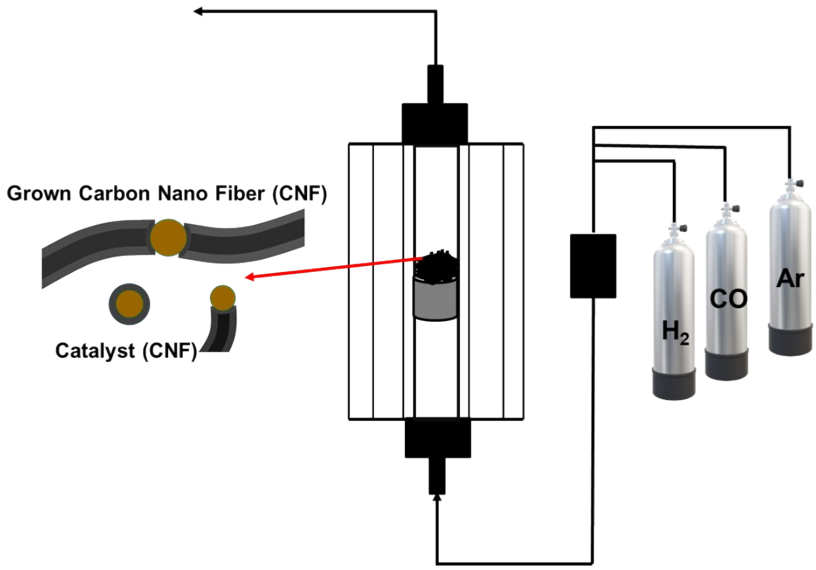

Experimental studies have demonstrated that using a gas mixture containing 90% CO and 10% H_2 across a temperature range of 350 °C to 700 °C facilitates substantial carbon deposition. Within this range, temperatures near 500 °C have proven especially reliable for capturing large quantities of carbon. Iron oxide (Fe_3O_4) catalysts have shown high activity under these conditions, promoting efficient CO conversion and yielding solid carbon with desirable physicochemical properties.

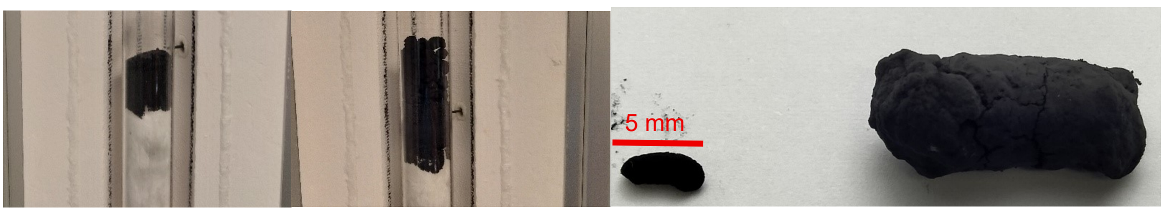

Figure S1. Before reaction (left) and captured after 1 h of HNC (right).

The synthetic yield of HNC increased almost linearly when the temperature was maintained at 500 °C and the gas flow rates were set at 2000 mL/min for CO and 200 mL/min for H_2. After 1 hour of synthesis, 9.7 g of HNC was collected over 0.5 g of catalyst grains (Fig.S1).

In total 120 L CO gas was spent and 9.7 g HNC captured. The yield was calculated using the Boudouard reaction ($2CO \rightarrow C + CO_2$). The yield was calculated to be approximately 30%.

$$CO \rightarrow \frac{C}{2} + \frac{CO_2}{2}$$

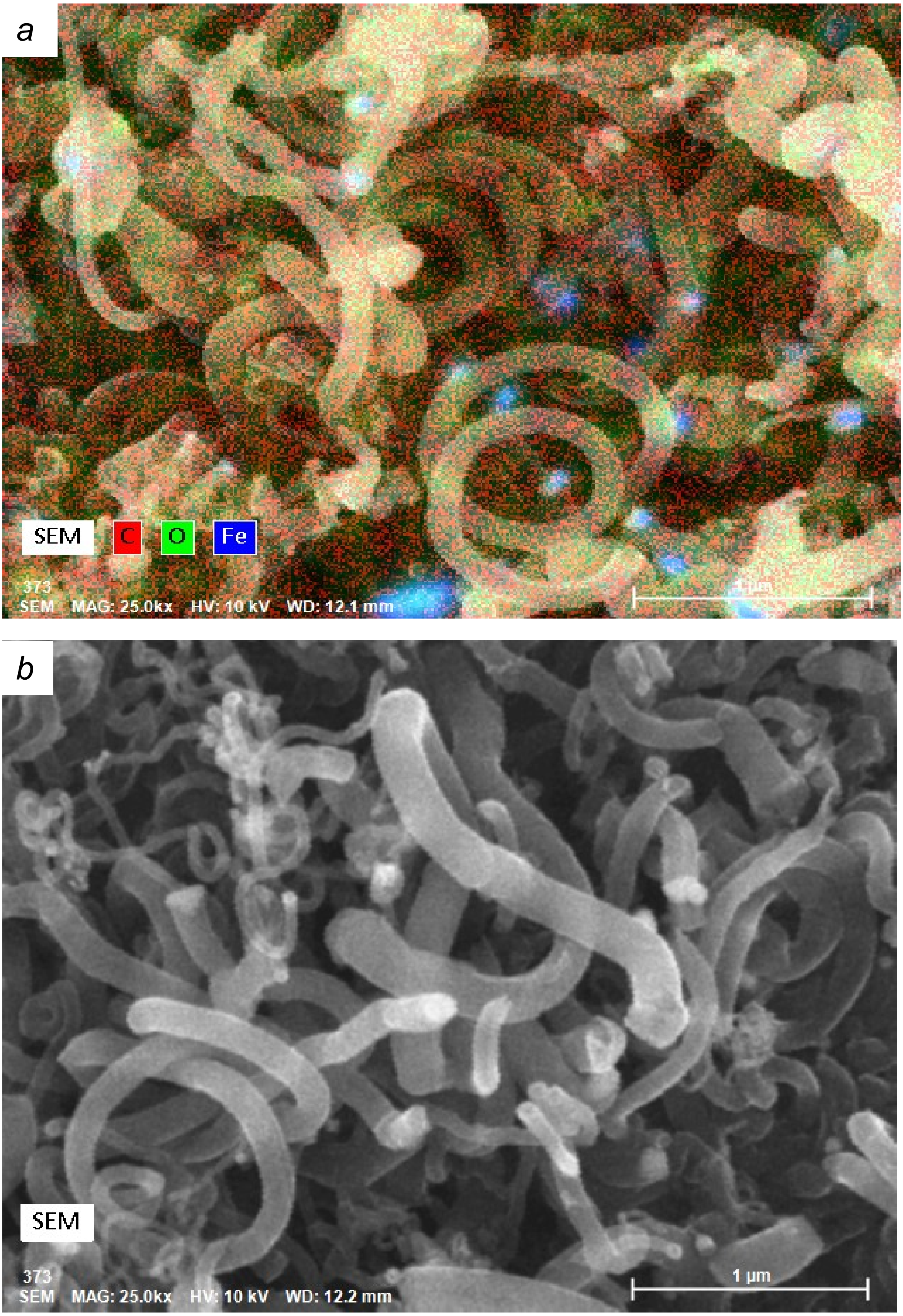

Figure S2. SEM micrographs of the HCN materials. Panels (a) and (b) present SEM images showing variations in surface morphology and pore structure.

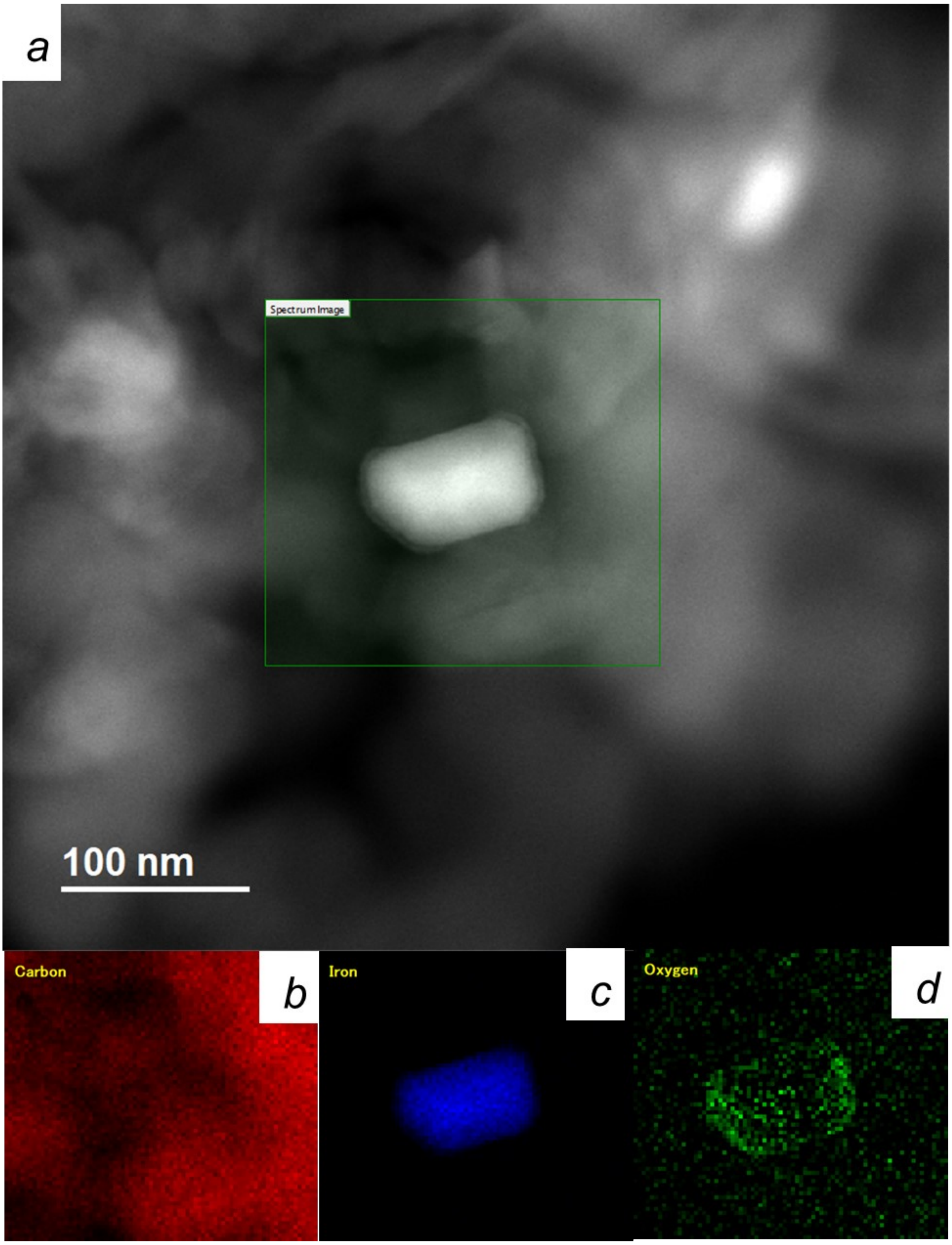

Figure S3. TEM micrographs of the HCN materials. TEM images illustrating internal structure, porosity, and nano structural changes. (*a*)presents the carbon growth region, highlighting the spatial distribution of the main elements: (*b*) carbon, (*c*) oxygen and (*d*) iron.

Scanning transmission electron microscopy (STEM) analysis further confirmed that these catalyst nanoparticles consist primarily of Fe and C, with a small amount of oxygen (Fig.3).

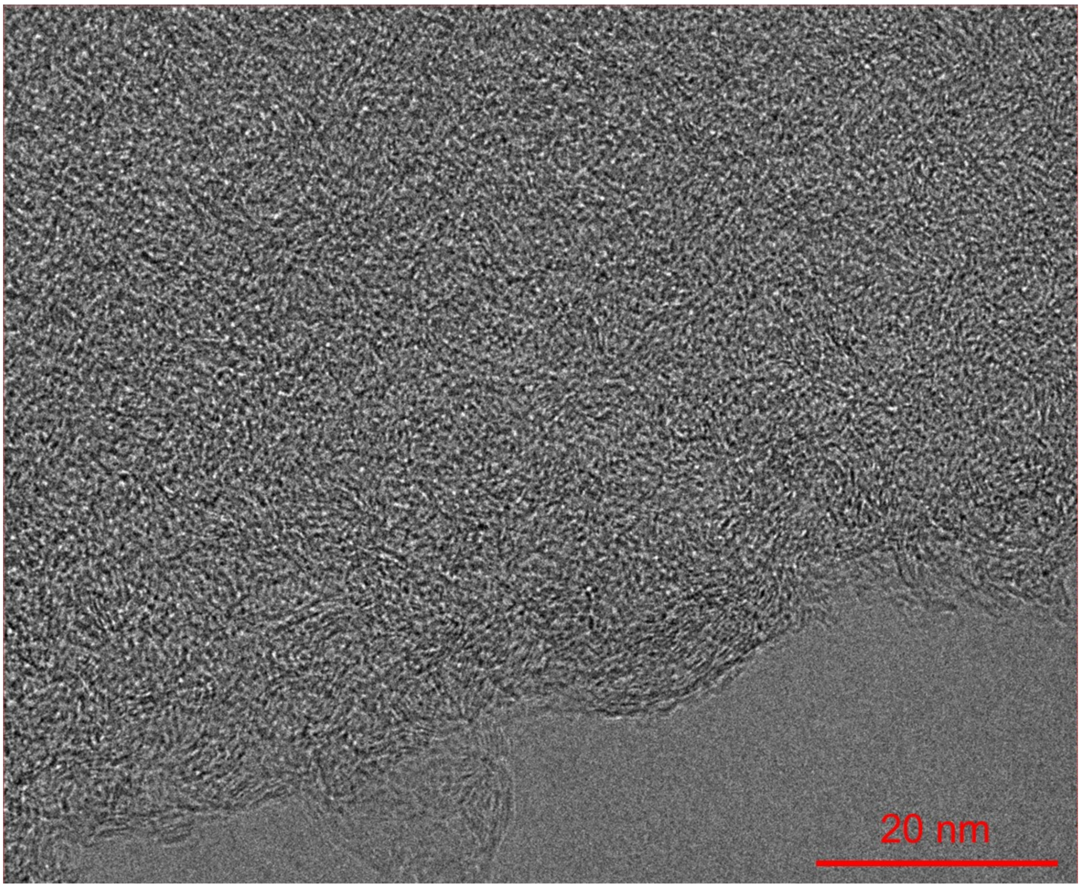

Figure S4: TEM image of the Activated Carbon (AC)

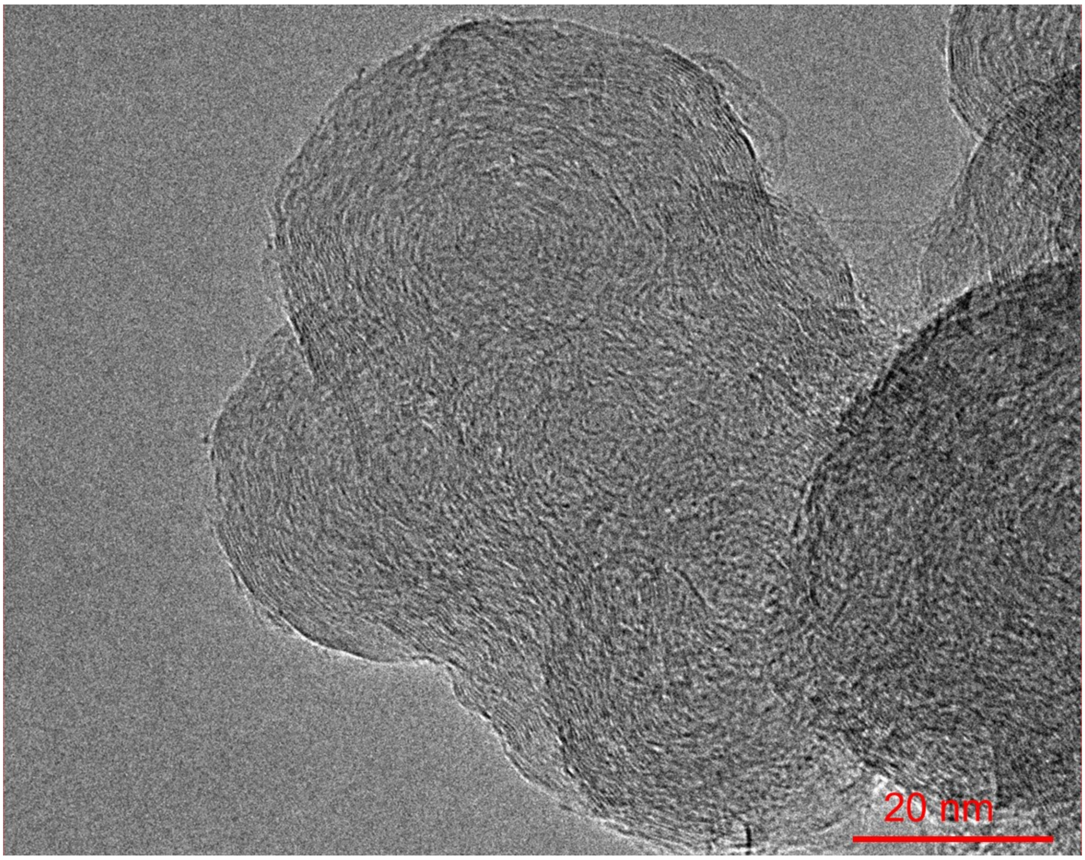

Figure S5: TEM image of the, Denka Li 400 (AB)

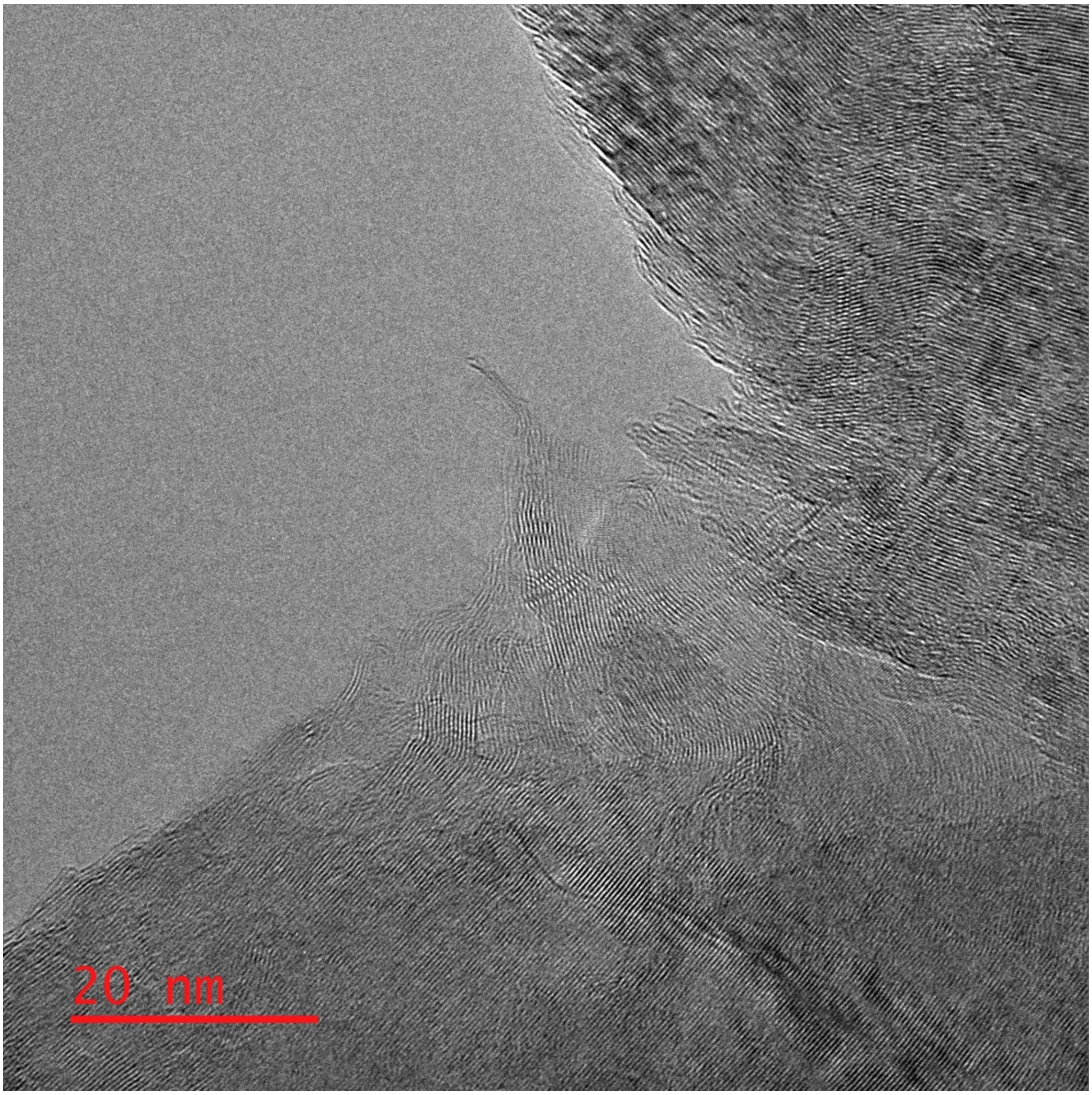

Figure S6: TEM image of HNC

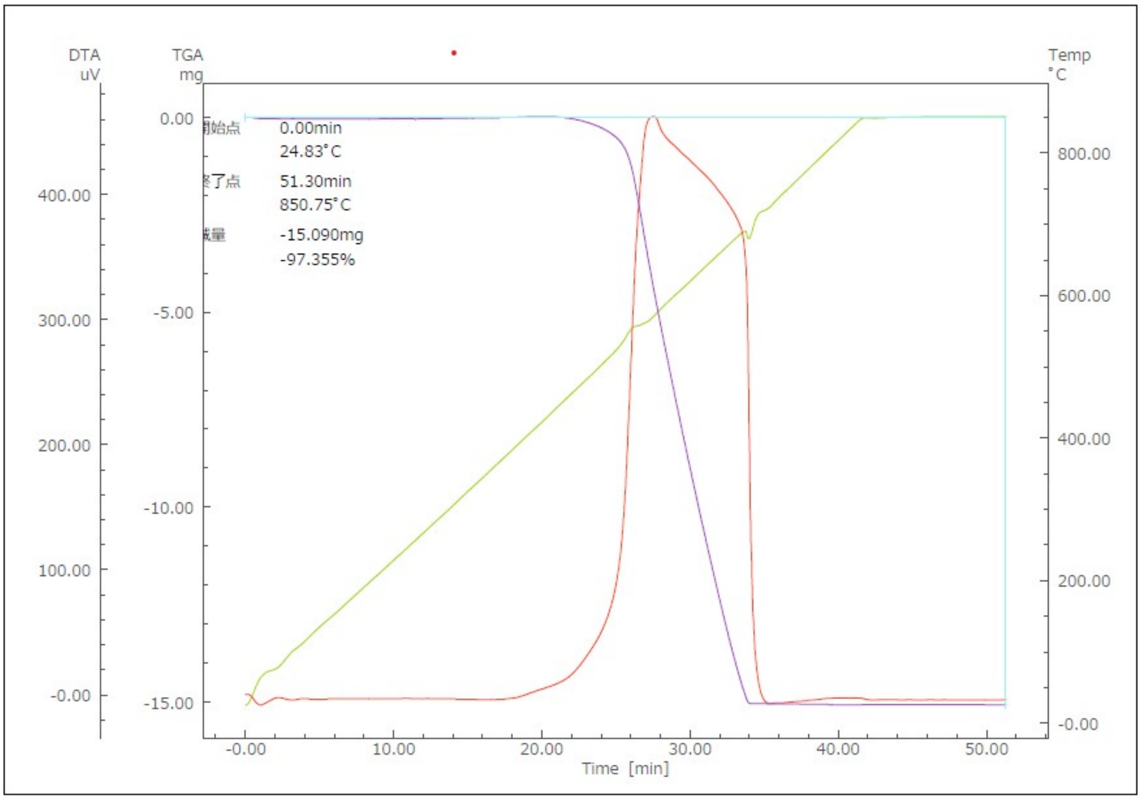

Figure S7. Thermogravimetric analysis (TGA) result of HNC under air flow at a heating rate of 20 °C min^{-1}.

The purity and thermal performance of the HNC were evaluated using TG/DTA (Thermogravimetric Analysis / Differential Thermal Analysis), Air atmosphere used to create an inert atmosphere during the analysis. The temperature was set to 850°C, and the target temperature was reached within 15 minutes. The air flow rate was maintained at 100 ml/min throughout the process, ensuring optimal conditions for accurate evaluation. Thermogravimetric/differential thermal analysis (TG/DTA) indicated that the Fe content in the HNC material was 2 $\pm$ 0.5 wt%.

Quantitative analysis of surface functional groups on HNC

0.5 g of sample was weighed into an Erlenmeyer flask and 80 ml of an alkaline aqueous solution of 0.05 mol/L sodium hydroxide, sodium carbonate, and sodium bicarbonate was added. The mixture was stirred in a nitrogen atmosphere and left to stand at room temperature to allow the sample to settle, and the filtrate was back-titrated with 0.05 mol/L hydrochloric acid. (For back titration, an automatic titrator AT-710WIN manufactured by Kyoto Electronics)

Table S1 Alkali consumption (mmol/g)

Sample name	NaOH	Na2CO3	NaHCO3
functional carbon	0.04	N. D.	N. D.

*Values below 0.01 mmol/g are indicated as "N.D."

Table S2 Surface functional group amount (mmol/g)

Sample name	Total acidic functional groups (NaOH consumption)	Carboxyl group (NaHCO3 consumption)	Phenolic hydroxyl group (NaOH consumption - Na_2CO_3 consumption)
functional carbon	0.04	N. D	0.04

Table S3 Optimization of Adsorption Parameters for Multiple Dyes

Dye	**Range Studied(mg/L)**	**Optimum Value(mg/L)**	**Removal Efficiency (%)**	**Adsorption Capacity (mg/g)**
RhB	40 – 160	80	88	35.1
Rh6G	40 – 160	40	83	16.7
Eosin Y	40 – 160	160	89	71.1
Rh 123	40 – 160	40	64	13

Adsorption Capacity (q) was calculated using the following equation:

$$q = \frac{(C_0 - C_e)\, V}{m}$$

Where:

- C_0 – initial dye concentration (mg/L)
- C_e – equilibrium dye concentration (mg/L)
- V – volume of the solution (L)
- m – mass of the adsorbent used (g)
- q – adsorption capacity (mg/g)

Each adsorbent (HNC and Activated Carbon) has its own q value, which represents how much dye is adsorbed per gram of material.

Table S4 Absorbance capacity q for HNC

Initial **(mg/g)**	Rh B **(mg/g)**	Rh 6G **(mg/g)**	Eosin Y **(mg/g)**	Rh 123 **(mg/g)**
20	20	16.7	20	12.7
40	35.1	18.6	40	12.4
80	46.8	31.2	71.1	10

Table S5 Absorbance capacity q for AC

Initial **(mg/g)**	Rh B **(mg/g)**	Rh 6G **(mg/g)**	Eosin Y **(mg/g)**	Rh 123 **(mg/g)**
20	9.6	12.4	9.2	12.9
40	21.8	15	17.5	39
80	19.3	11.2	24.8	36

Table S6 Comparison of the adsorption capacity of HNC with other adsorbents.

Adsorbent	RhB (mg L-1)	pH	Adsorption efficiency values %	Reference
Carbon graphite (KS44-0)	2.5	3	55	[1]
C. lawsoniana sundried powdered fruit	40	2	85	[2]
Spent tea leaves	20	3	14	[3]
Pinecone charcoal	75	2.4	80	[4]
Causuarina equisetifolia needles	20	4.4	85	[5]
HNC	40	2.75	97	This work
HNC	40	3.84	96	This work
HNC	40	4.63	98	This work
HNC	40	6.63	92	This work
HNC	40	10.5	87	This work

Water purification performance

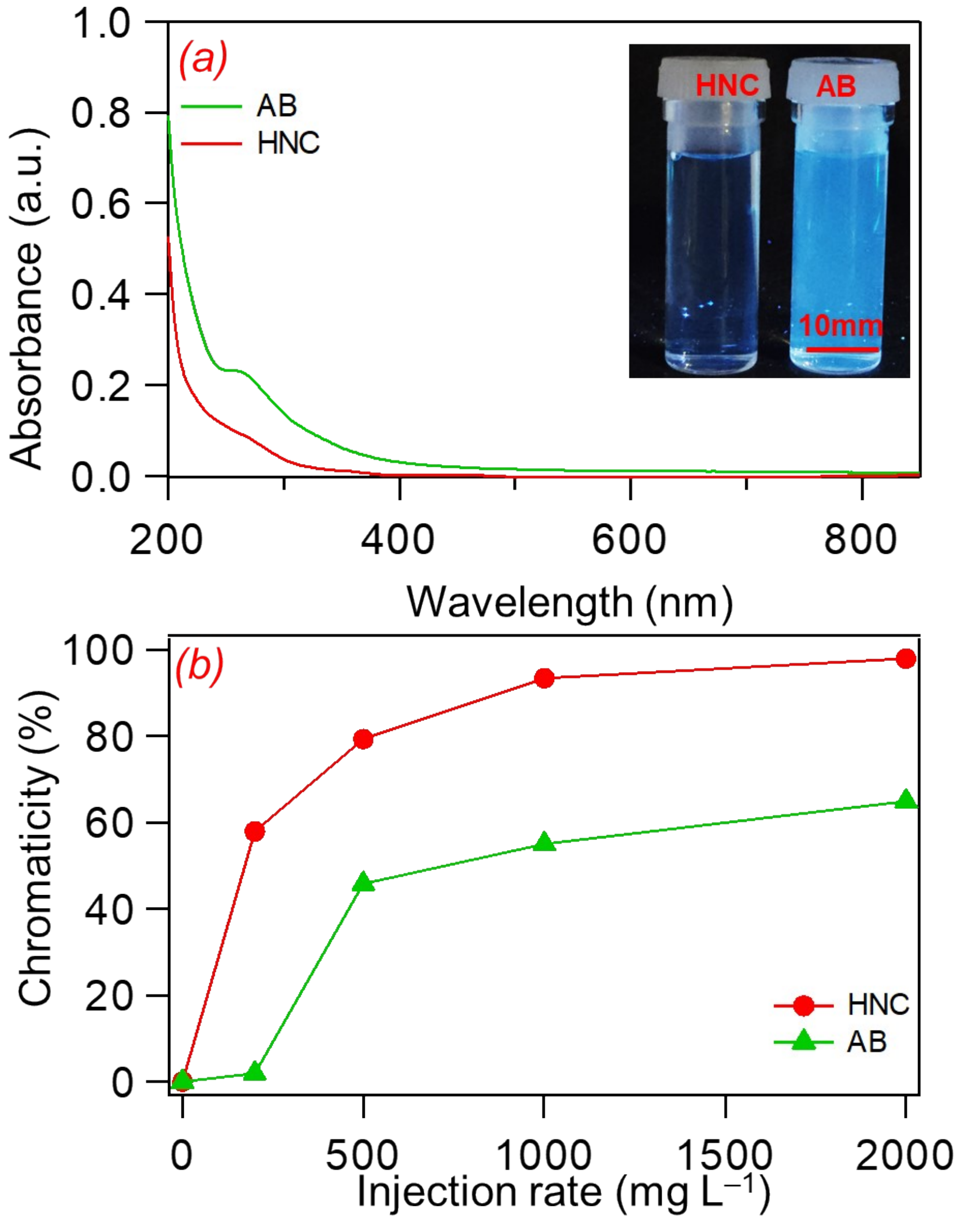

Figure S8. *(a)* UV–VIS spectra for actual Wastewater after purification with Acetylene Black (AB, Denka Li 400) and HNC (dose of 2000 mg L^{-1}), *(b)* Chromaticity at a wavelength of 390 nm as a function of the injection rate of carbon adsorbents.

The decolorization efficiency of HNC was evaluated at increasing doses (200, 500, 1000, and 2000 mg L^{-1}). For AB, the corresponding chromaticity values were %, 46 %, 55 %, and 65 %, whereas for HNC, the values were 58 %, 80 %, 94 %, and 98 %, respectively (Fig. S8). These results confirm that HNC is an effective alternative to commercial AB for wastewater treatment.

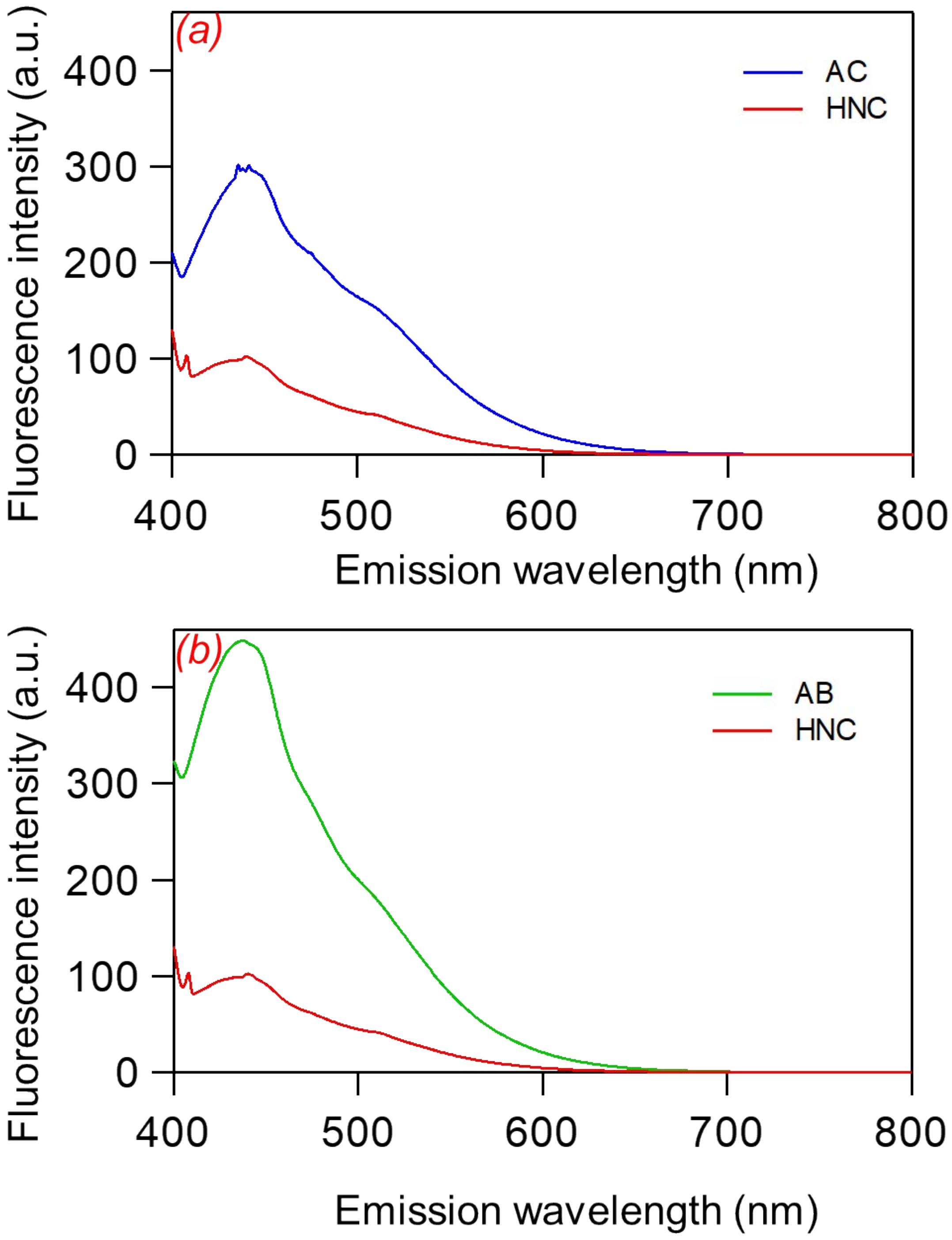

Figure S9. Emission spectra at 350 nm excitation of purified water: (*a*) water treated with AC and HNC, and (*b*) water treated with AB and HNC.

Fluorescence spectra of actual domestic wastewater after purification and analysis at excitation wavelength λ_{ex}=350 nm using a spectrofluorometer. Measurements were made by placing 2 mL of each sample in a quartz cell. (*a*) Wastewater treated with AC and HNC. (*b*) AB and HNC. Experimental results obtained at a dose of 2000 mg L^{-1}.

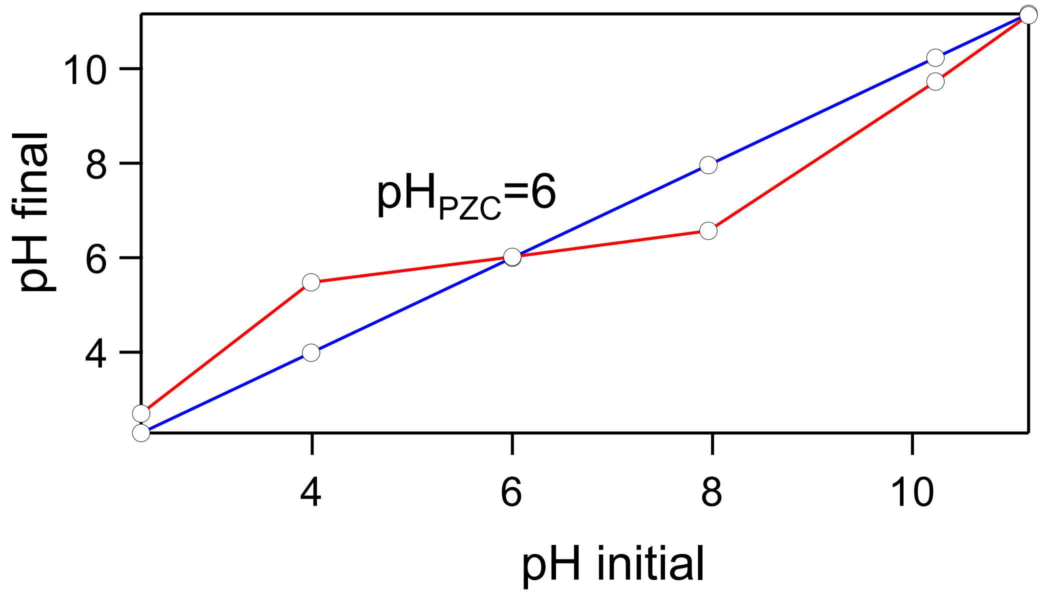

Figure S10. Determination of the Point of Zero Charge (pH_{pzc})

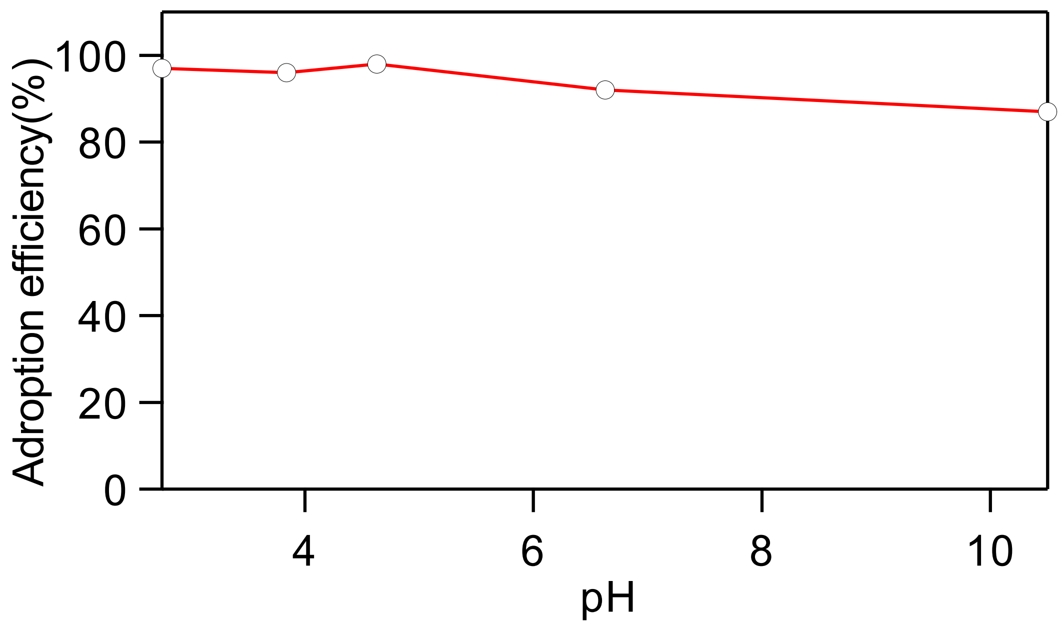

Figure S11. Effect of pH on RhB dye removal. The experimental conditions included dye concentration = 40 mg/L, time = 2 min, at room temperature ◦C, pH = variable (2 - 10), and adsorbent dosage = 0.02 g.

Table S7. Effect of pH on RhB dye removal efficiency of HNC. Initial concentration was 40 mg L^{-1}.

pH	Removal efficiency (%)
2.75	97
3.84	96
4.63	98
6.63	92
10.5	87

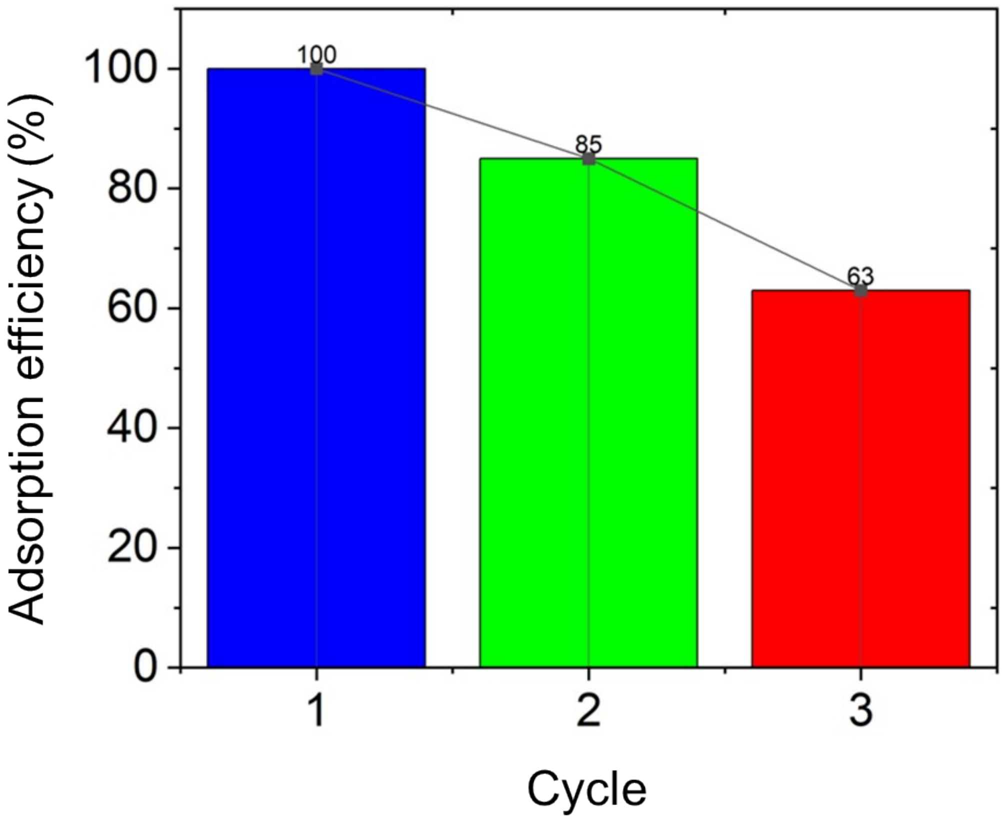

Figure S12. Recycling experiment.

To evaluate the stability and reusability of the carbon adsorbent, the material was subjected to consecutive adsorption–desorption (washing) cycles. After each cycle, the carbon was carefully washed, dried, and weighed. The mass loss during each cycle was calculated using the following equation:

Mass loss (%) = $\frac{m_0 - m_n}{m_0} \times 100\%$

where:

- $m_0$is the initial mass of the carbon before reusing,
- $m_n$is the mass of the carbon after the n-th washing cycle.

Fresh HNC was 2 g and dried spent was 1.735g. The results showed that the mass loss during each cycle was around 15%.

Table S8. Physicochemical parameters of real domestic wastewater.

Parameters	Wastewater sample
Chemical oxygen demand (mg L^{-1})	120
Amount of suspended solids (mg L^{-1})	200
Nitrogen content (mg L^{-1})	21
Phosphorus content (mg L^{-1})	3.4
Hydrogen ion concentration (20.9℃) pH	7.7

Chemical oxygen demand (COD) concentration was determined by analyzing the oxygen demand by potassium permanganate at 100°C (COD Mn) (JIS K0102 17). Total nitrogen (TN) concentration was determined by ultraviolet absorption photometry (JIS K0102 45.2) and total phosphorus (TP) concentration was determined by potassium peroxydisulfate resolution method (JIS KO102 46.3.1). Hydrogen ion concentration (pH) was determined using the glass electrode method by measuring the potential difference after immersing the electrode in the sample (JIS K 0102 12.1). Suspended solids (SS) concentration was determined by the gravimetric (filtration) method, in which the sample was filtered, and the retained residue was dried and weighed (JIS K 0102; Environmental Agency Notification No. 59).

References

1. Zghal, S., Jedidi, I., Cretin, M., Cerneaux, S., & Abdelmouleh, M. (2020). Adsorptive removal of Rhodamine B dye using carbon graphite/CNT composites as adsorbents: Kinetics, isotherms and thermodynamic study. Materials, 13(6), 1344.
2. Gul, S., Gul, H., Gul, M., Khattak, R., Rukh, G., Khan, M. S., & Aouissi, H. A. (2022). Enhanced adsorption of Rhodamine B on biomass of Cypress/False Cypress (Chamaecyparis lawsoniana) fruit: Optimization and kinetic study. Water, 14(19), 2987.
3. Donatto, A.E.; Nascimento, M.S.; Lourenço, J.B.; da Silva,W.L. Study of adsorption of Rhodamine B dye using the residual biomass of mdf and porongo. Int. J. Sci. Res. 2019, 10, 31158.
4. Thakur, A.; Kaur, H. Removal of hazardous Rhodamine B dye by using chemically activated low cost adsorbent: Pine con charcoal. Int. J. Chem. Phys. Sci. 2016, 5, 17–28.
5. Kooh, M.R.R.; Dahri, M.K.; Lim, L.B. The removal of Rhodamine B dye from aqueous solution using Casuarina equisetifolia needles as adsorbent. Cogent Environ. Sci. 2016, 2, 1140553.